Growth of breakdown susceptibility in random composites and the stick-slip model of earthquakes: Prediction of dielectric breakdown and other catastrophes

Muktish Acharyya* and Bikas K. Chakrabarti[†]

Saha Institute of Nuclear Physics, 1/AF Bidhannagar, Calcutta 700 064, India

The responses to short duration pulses (of electric field, of additional "particles," of a mechanical "push due to blasting" on any "tectonic block," etc.) have been studied numerically for metal-insulator composites before dielectric breakdown, the Bak-Tang-Weisenfeld (BTW) (sandpile) model before the critical avalanches, and the Burridge-Knopoff stick-slip model of earthquakes. We show that, from the response to weak pulses of appropriate external field, one can estimate the growth of local failure correlations in such systems, giving the breakdown susceptibility. The study of this breakdown susceptibility, contributed to by the correlations of microscopic local failures, indicates universal behavior near the catastrophic (global) breakdown or the self-organized critical points. Its study can thus help in accurately locating the global breakdown or disaster point (much before its occurrence) by extrapolating the inverse breakdown susceptibility to its vanishing point. We have performed numerical studies of Laplace's equation of a dielectric with random bond conductors below its percolation threshold, of the dynamics of the BTW model, and of the dynamical equations of the array of blocks in the stick-slip model of earthquakes. The breakdown susceptibility has a power law growth (with the critical interval from the global breakdown threshold) in both the electric breakdown and in the BTW model. Accurate exponent values for the growth have been obtained in the BTW case. The growth of the susceptibility, coming from stress correlations, in the Burridge-Knopoff model of earthquakes is observed to be exponential in time, as it is for pulse susceptibility in this model.

PACS number(s): 05.45.+b, 05.40.+j, 91.30.Px

I. INTRODUCTION

Considerable progress has recently been made in the statistical study of the breakdown strength of disordered solids [1]. These solids may be porous media, random composites, granular packings, or layers in the earth's mantle; the relevant phenomena are fractures, dielectric breakdowns, avalanches, or earthquakes. Several simple models (at a semimicroscopic level) have been introduced for mechanical [2] and electrical [3] failure of such randomly disordered media, where the media are represented by disordered lattices and the failure is modeled by individual bonds breaking irreversibly. These theoretical results about the fracture or breakdown strength distribution have also been checked in several experiments [4]. Recently, there have been important extensions of these electrical failure models [3] of randomly disordered media to the electromigration failures in microscopic thin film circuits [5]. Also the stick-slip model of Burridge and Knopoff [6] for earthquakes has been studied extensively in recent times [7] to investigate the failure properties in earthquakes.

Because failure processes play intrinsic roles in many systems of industrial importance and in many natural disaster phenomena, the above mentioned statistical studies establishing the nature of fracture-strength or earthquake magnitude distributions and their fluctuations [1] are of extreme importance. Although a significant amount of literature has been developed for these studies of failure strength distribution, not much has been done on the dynamics of microscopic failures. Since the microscopic failures are irreversible and therefore require intermediate redistributions of the forces, the equations for the dynamics of failure are intrinsically nonlinear and dissipative. The formulation and study of such equations are necessary for the search of any precursor effect of the macroscopic failure. In some recent experiments [8] on the dynamics of the cracks in thin glass plates with thermal stresses, the dynamics seems to undergo a sequence of numerous but reproducible instabilities that is not sensitive to every detail of the fluctuations in the initial conditions. The dynamics of fractures is thus observed to be mostly critical, on the verge of chaos but not quite chaotic [9]; the situation depends somewhat on the velocity of the crack tip. Similar is the case for the dynamical models of earthquake [7], where also one gets the Gutenberg-Richter-type power law for the magnitude variation of the density of quakes, the failure distribution being critical.

All these studies establish the very nonlinear, yet non-chaotic (but on the edge of chaos), nature of the dynamics of breakdowns. This absence of full-grown chaos suggests the possible existence of correlations until the (global) breakdown point. Very recently, the computer simu-

*Electronic address: muktish@saha.ernet.in
†Electronic address: bikas@saha.ernet.in

lation study of the local dynamics of failures in these models [2,3,6] has indicated [10] a novel correlation of local failures. These correlations grow (often critically) as the macroscopic or global breakdown point (for example, the earthquake point) is approached. It has been seen [10] that suitable short-duration pulsed perturbations can sense these growing correlations. From the study of response behavior (to such pulses), knowledge about the growth of the breakdown susceptibility can therefore be obtained. This growing (breakdown) susceptibility may be studied and viewed as a precursor effect, and its knowledge can help early predictions of the catastrophes.

Here, we have studied in detail these growing correlations of local failures and the consequent growth of breakdown (or failure) susceptibility as the global breakdown point is approached in the above mentioned (well-studied and established) models for failures (breakdown) in random composites or in earthquakes. We also study how the response of such systems to appropriate pulsed perturbations can give the information regarding this growing breakdown susceptibility, and thereby help in predicting the imminent catastrophes (in these models). We have also checked such prediction possibilities for the self-organized critical (SOC) point in the Bak-Tang-Weisenfeld (BTW) model [11]. In particular, we study here the response to electric pulses and the growth of the local or breakdown susceptibility in a metal-insulator composite (a dielectric with randomly placed conducting sites). This is done numerically (following essentially Manna and Chakrabarti [12]) by solving Laplace's equation for a random nonpercolating lattice network of conductors. We find that the rate of local failures (the number of dielectric bonds that break because the terminal voltage goes beyond their threshold value), per unit increase of voltage across the sample, increases sharply and finally diverges at the critical breakdown voltage of the sample. This gives the breakdown susceptibility. A similar study has been made to investigate the avalanche susceptibility (contributed to by the local avalanches in the SOC dynamics) in the BTW model. We have determined here the avalanche or breakdown susceptibility exponent (or the dynamic exponent) value accurately for the BTW model (in dimension $D = 2$). We then study the growth of breakdown susceptibility in the Burridge-Knopoff stick-slip model of earthquakes where local pulsed momentum is given periodically at any particular block. We look for its (the same block's) strain displacement periodically, by solving numerically (using the fourth-order Runge-Kutta method) the dynamical equations of motion of the system. The pulse susceptibility again tends to diverge at the earthquake point. The same behavior is also observed for the susceptibility coming from the stress-stress correlations of the blocks of the unperturbed system. Knowledge about the growth of these (breakdown) susceptibilities (obtained from the response to appropriate pulses) can therefore help one to predict the (global) catastrophic points (time) by studying the decay of inverse susceptibilities before the global breakdown and extrapolating to its vanishing point.

We organize this paper as follows: In Sec. II, we have described the results of our numerical simulation to esti-

mate the breakdown voltage in a random metal-insulator composite by searching the macroscopic connection via conducting sites. The same has also been obtained from the location of the peak of the breakdown susceptibility and compared. Section III contains the computer simulation results for the avalanche susceptibility and the estimate of the dynamic exponent of SOC in the BTW model. The results about the breakdown susceptibility (and prediction of the earthquake point) in the Burridge-Knopoff model for earthquakes by solving the dynamical equation of motion, are discussed in Sec. IV. The paper ends with concluding remarks and a summary in Sec. V.

II. GROWTH OF BREAKDOWN SUSCEPTIBILITY AND PREDICTION OF BREAKDOWN VOLTAGE

To study the dielectric breakdown property [12] of a random mixture of conductors and insulators (dielectrics), we consider now an $L \times L$ square lattice, with $L = 25$. A fraction p_0 of its sites are randomly occupied using a Monte Carlo program; they represent conducting sites before breakdown starts. The $(1 - p_0)$ fraction of unoccupied sites represents the dielectric sites. For each configuration with average conductor concentration p_0 ($< p_c$, p_c representing the percolation threshold [13], with $p_c \cong 0.593$), we first check whether or not there exists any percolating path through the preexisting conducting sites. Percolation connections are taken here through the nearest-neighbor conductor sites in the sample. If no such path exists, giving the macroscopic connection across the lattice, we apply a voltage VL across the sample in the horizontal direction, with all sites at the leftmost column at zero voltage and those at the rightmost column at voltage VL. We then update the site potential by using the following steps:

(i) All the sites (except the conducting boundary sites) are first given a random value of potential.

(ii) We update the chosen site potential according to the solution of the discretized Laplace's equation for the field potential. The new value of the field at a particular site (i,j) will be

$$V(i,j) = \frac{V(i+1,j) + V(i-1,j) + V(i,j+1) + V(i,j-1)}{4}$$

in a square lattice.

(iii) All the nearest-neighbor conducting sites (of that chosen site, if it is conducting) are then updated to the same potential (field), which is the arithmetic mean of the earlier values of the potential of those sites.

(iv) We keep on updating each lattice site at each iteration over the lattice until the sum of the differences of potentials of all sites in the successive updates goes below a small value (10^{-4} here).

(v) We than check if any two neighboring sites have a potential difference beyond a preassigned threshold v_c value (1.0 here), when we consider the corresponding (dielectric) bond as broken, and two terminal sites are then permanently replaced by (newly added burned) conductors.

Following these updating rules, we have calculated the

minimum voltage required (for a particular initial conductor concentration) to get a macroscopic connection via the (original and burned) conducting sites. This value of the potential is called the breakdown voltage for that particular initial conductor concentration. We take the average $V_b^p(p_0)$ over various initial configurations (typically 1000 configurations here) as the percolating breakdown field at the (initial) conductor concentration p_0. It is clear that the average breakdown voltage for a fixed sample of dimension L decreases with increasing initial conductor concentration p_0, until it vanishes at the percolation threshold p_c [13]. For any particular initial concentration p_0 of random conductors, the sample dielectric has an average (percolation) breakdown field (voltage per unit sample length L) $V_b^p(p_0)$, above which the sample starts conducting (percolating) via the conductors (original and broken). This variation of $V_b^p(p_0)$ is shown in Fig. 1. It may be noted here that $V_b^p(p_0)$ represents the final breakdown field, at which the broken system just percolates via the conducting bonds (original and broken dielectrics). As such, it differs from the breakdown initiation field (at which one dielectric bond breaks) studied in Ref. [12].

We intend to predict this $V_b^p(p_0)$ value by looking at the response of the sample to electrical fields (pulses) much before its global or percolation (through original and burned conductors) breakdown occurs. For this, we make an increase dV, over V [for $V \ll V_b^p(p_0)$], in the applied voltage across the sample and look for the number (n) of dielectric bonds breaking locally (or conducting sites newly created as the voltage across the dielectric bonds goes beyond the threshold value $v_c = 1.0$). This helps us to define the breakdown susceptibility $\chi_d = dn/dV$. It is shown in Fig. 2 for three different initial conductor concentrations, $p_0 = 0.5$, 0.4, and 0.3 (averaged over 5000 initial configurations). The maximum of

FIG. 2. Variation of breakdown susceptibility χ_d with applied field (V) across the sample for various initial conductor concentrations (p_0). Inset shows the variation of breakdown fields (voltage per unit of sample length) $V_b^\chi(p_0)$, obtained from the peak position of χ_d, and $V_b^p(p_0)$, obtained from the percolation due to breakdown (Fig. 1), with initial conductor concentration p_0. Here system size $L = 25$.

χ_d gives the possible location of breakdown voltage. The peak in χ_d occurs at the field strength (voltage per unit of sample length) $V_b^\chi(p_0) \cong 0.44$, 0.34, and 0.26 for $p_0 = 0.3$, 0.4, and 0.5, respectively, for fixed sample size $L = 25$. These values may be compared to those obtained from the direct percolation breakdown voltage in this model: $V_b^p(p_0) \cong 0.558$, 0.385, and 0.097 for $p_0 = 0.3$, 0.4, and 0.5, respectively, for the same sample size $L = 25$ (when the
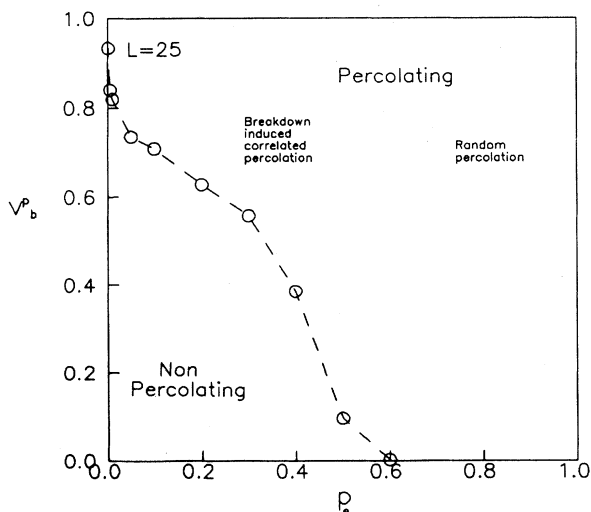

FIG. 1. Variation of the average percolation breakdown electric field $V_b^p(p_0)$ with the initial conductor concentration p_0 for sample size $L = 25$.
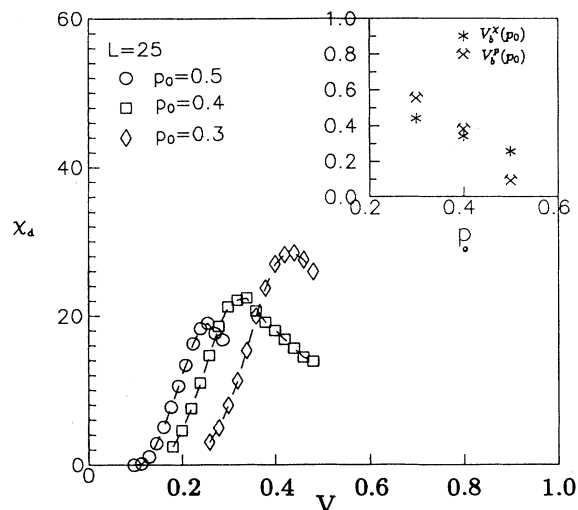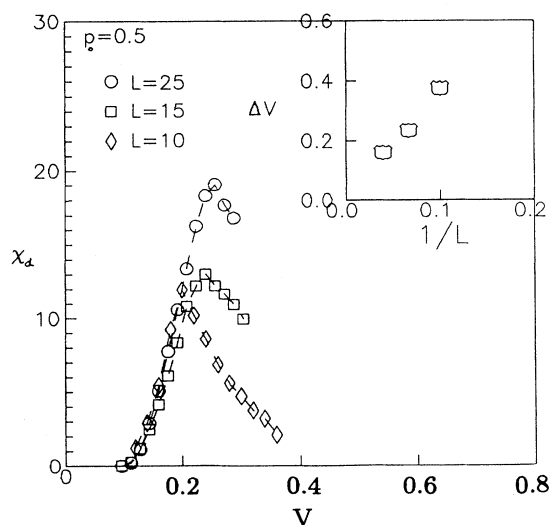

FIG. 3. Variation of χ_d with respect to the applied field (V) across the sample for various system sizes (L) and a fixed initial conductor concentration $p_0 = 0.5$. The inset shows the variation of $\Delta V \equiv V_b^\chi(p_0) - V_b^p(p_0)$ with the system size.

applied electric field is above the breakdown voltage and conductors percolate through broken dielectric bonds). It may be noted that the peak in χ_d increases in height with the system size L, as can be seen from Fig. 3. Here the inset shows that the difference $\Delta V \equiv V_b^p - V_b^\chi$, in the breakdown field estimates from the percolation and susceptibility χ_d, decreases with L^{-1}. Thus an extrapolated point where χ_d^{-1} vanishes gives the predicted location of the breakdown voltage. In fact, since the extra conductors, coming from burned dielectrics, will change the dielectric constant of the sample, χ_d can be estimated from the measurement of the dielectric constant of the composite material.

III. AVALANCHE SUSCEPTIBILITY IN THE BTW MODEL

We consider now the self-organized criticality of the critical "height" BTW model [11], considered to be a generic cellular automata model of self-tuned (or self-organized) avalanche dynamics in sandpiles and earthquakes. We consider a lattice size of 100×100. At each lattice point the "heights," or "particles," are randomly added in discrete integer addition and avalanches take place if the height Z_i at any point i exceeds the value 3 (the cutoff value $Z_0 = 4$). In such cases, the $Z_{i+\delta}$ of the nearest neighbors δ of the site i gets one unit of height each and Z_i becomes zero at i. The dynamics continues, until all the sites have $Z < 4$. The simulation studies give the value of the average critical height Z_c to be around 2.124 [14] for such a model, beyond which the global avalanches take place.

We have studied the effect of the addition of a fixed (small) number h_p of particles (or heights) at any central point for a time unit δt, when the system has reached the average height $\bar{Z}(< \bar{Z}_c)$ and the dynamics (before the addition of these particles) has stopped. Immediately after the particles are added, the local dynamics starts again, and it continues for a time period $\Delta t(\geq \delta t)$. We measure the ratio $R = \Delta t / \delta t$ of the response time to the perturbation (pulse) time. We find that $R \sim (Z_c - \bar{Z})^{-\gamma}$, where $\gamma \cong \frac{1}{3}$ (see Fig. 4). It may be noted that γ is the dynamic exponent in this case. One can thus precisely estimate the value of $\bar{Z}$ at the self-organized critical point (or critical height) Z_c by plotting $R^{-1/\gamma}$ with $\bar{Z}$ and by locating its vanishing point, which gives $Z_c \cong 2.16$. This is indeed very close to the previous straightforward numerical estimate $Z_c \cong 2.124$ [14] in the model.

Like the growth of response time (Δt for fixed perturbation time δt), with approach to criticality ($\bar{Z} \rightarrow \bar{Z}_c$) in the BTW model (as studied above), the size (length) of the perturbed region (for an additional pulse of height at a fixed site) also increases as $\bar{Z} \rightarrow \bar{Z}_c$. To have a quantitative measurement, we have studied the number $N_s(\bar{Z})$ of sites affected (toppled at least once) because of a fixed addition of particles (height) at a particular (central) point in the BTW model. This $N_s(\bar{Z})$ is also seen to diverge as the average height $\bar{Z}$ approaches the critical point $\bar{Z}_c$. In fact, we have found $N_s^{-\Delta} \sim (\bar{Z} - \bar{Z}_c)$, with $\Delta \cong \frac{1}{2}$. Figure 5 shows the variation of $N_s^{-\Delta}$ with $\bar{Z}$, which is indeed a
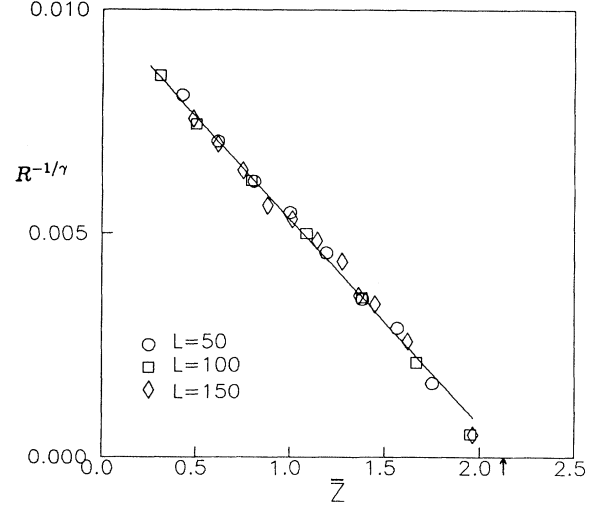

FIG. 4. Variation of $R^{-1/\gamma}$ with $\bar{Z}$; $h_p = 10$, $\delta t = 10$ time iterations, and $L = 100$. We have fitted $\gamma = \frac{1}{3}$.

straight line. The extrapolation of this straight line gives the estimate of $\bar{Z}_c$. The accuracy of the estimate of $\bar{Z}_c$ increases as both the duration δt and the size h_p, or in other words the magnitude of perturbation ($= h_p \delta t$), decreases (see the inset in Fig. 5).

IV. NATURE OF RESPONSE TO PULSES AND POSSIBLE PREDICTION OF CATASTROPHES IN MODEL EARTHQUAKE SYSTEM

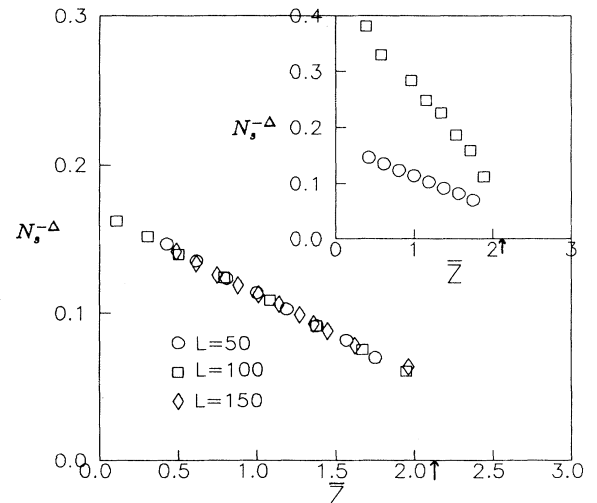We now study the stick-slip model [7] of earthquakes numerically [8]. In this model, a linear array of N blocks,

FIG. 5. Variation of $N_s^{-\Delta}$ with $\bar{Z}$ for different system sizes and for fixed $h_p = 10$ and $\delta t = 10$ time iterations. We have fitted with $\Delta = \frac{1}{2}$ here. The inset shows the variation of $N_s^{-\Delta}$ with $\bar{Z}_c$ for ($\bigcirc$) $h_p = 10$, $\delta t = 10$ time iterations, $L = 50$, and ($\square$) $h_p = 4$, $\delta t = 5$ time iterations, $L = 50$.

each coupled to its nearest neighbors by elastic springs and each connected to a rigid support (at the top) by elastic springs, is put on a uniformly moving rough platform. The equations of motion (after linear scale transformation) for any of the blocks, in the uniform spring constant Burridge-Knopoff model (Carlson-Langer [8]), can be written as

$$d^2 U_j / dt^2 = l^2 (U_{j+1} - 2U_j + U_{j-1})$$

$$- U_j - \phi[2\alpha v + 2\alpha (dU_j / dt)] , \qquad (1)$$

where U_j denotes the displacement of the jth block from its equilibrium position, l^2 is the ratio of the spring constants, α is a constant (linear transformation factor), and v is the uniform pulling velocity of the rough (frictional) platform. The nonlinear friction force is given by the function $\phi(y) = \text{sgn}(y/1 + |y|)$.

In such dynamical models, the elastic stresses (energy) developed completely with the (velocity dependent) frictional force as long as the blocks stick to the moving platform. As it fails, there occur local failures (slippage for a finite number of blocks) or global failures (simultaneous slippage of almost all the blocks). Initially the (elastic) energy increases and then suddenly falls (causing an avalanche or quake), releasing the excess elastic energy. As the released energy is often more than the "excess," the system again becomes "subcritical." The energy starts to build up again and after some time it falls, and the process continues. The strain energy released in any such failure is identified as the magnitude (strength) of the earthquake in this model system. We have solved the above set of equations by using the fourth-order Runge-Kutta method, taking 100 blocks ($N = 100$; $dt \sim 2^{-7}$). We have checked the distributions of earthquakes (the Guttenberge-Richter law) for the model and reproduced the previous results [7] for various initial randomness of the block velocities and positions. We then apply very weak pulses to an arbitrarily chosen (central, kth) block (giving fixed arbitrary $\delta U_k = 0.01$ for a duration $\delta t = 10 \times dt$; $k = 50$) at a regular time interval of $T = 1000 \times dt$. We then calculate again the total elastic energy $E_T (= \sum_j \{l^2/2[(U_{j+1} - U_j)^2 + (U_{j-1} - U_j)^2] + U_j^2/2\})$ at each time step and plot them against time [Fig. 6(a)]. In all the figures we show the typical results for $N = 100$, $l = 10$, $\alpha = 2.5$, and $v = 0.01$, although the general features we discuss are observed for many combinations of these parameter values within the range of parameter values for the numerical solution of (1), which gives power law behavior [7]. We also show in Fig. 6(b) the time variation of the elastic stress, ΔU_k $[= l^2(U_{k+1} - 2U_k + U_{k-1}) - U_k]$, developed on the kth block, on which the pulses are being applied. We also compare there [Fig. 6(c)], the time variation of the pulse susceptibility for earthquake χ_e, defined as $\chi_e = \Delta U_k^m / U_k^p$, with ΔU_k^m denoting the maximum of ΔU_k within the pulse period and $U_k^p = \int_0^{\delta t} \delta U_k dt$. We find $\chi_e \sim \exp[A(t_{c_n})/(t_{c_n} - t)]$ for $t < t_{c_n}$, where $A(t_{c_n})$ is a constant and t_{c_n} denotes the onset time of the nth earthquake or catastrophe. See Fig. 7 for an enlargement of

the correspondence of the χ_e peak and the earthquake in the model. It may appear [from Fig. 6(c)] that $(\ln \chi_e)^{-1}$ finally saturates to a fixed value (around 0.25) before the earthquakes. However, this is seen to be a finite size effect (see the following discussion on χ), and this saturation value vanishes as the system size N increases and goes to infinity.
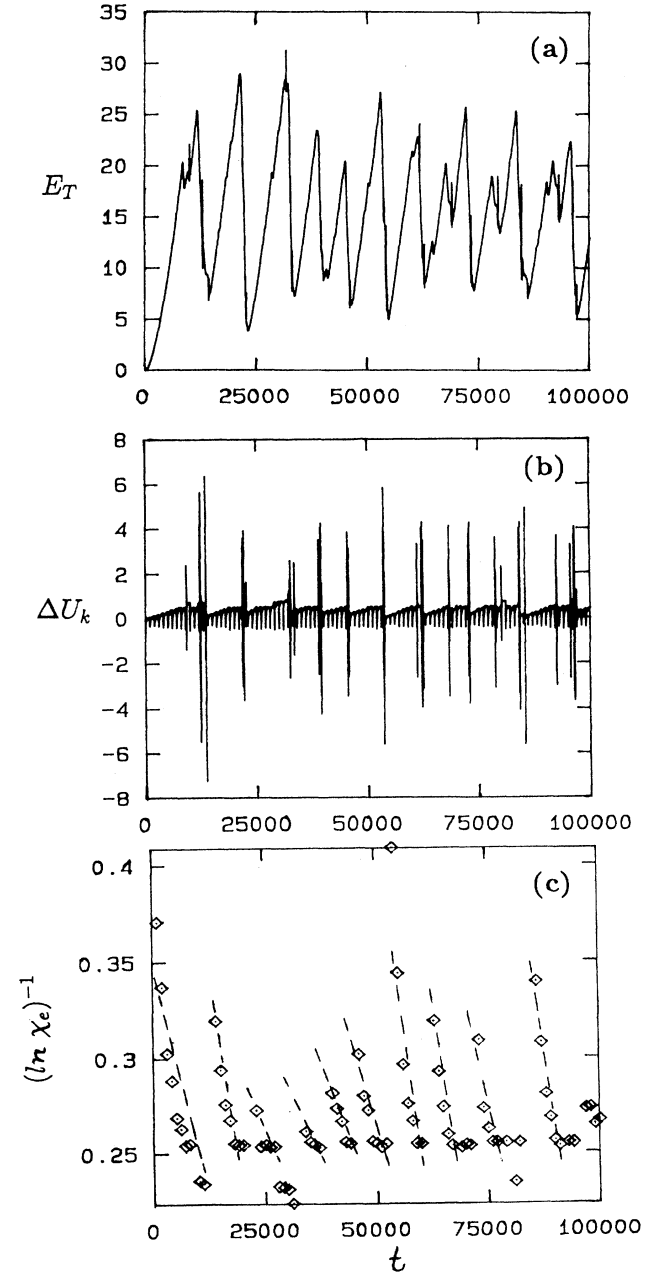
The growth of stress correlation in the same model

FIG. 6. Time variation of (a) total elastic energy E_T, (b) stress ΔU_k developed on kth block at which pulse has been applied, and (c) $(\ln \chi_e)^{-1}$. Here, $N = 100$, $\alpha = 2.5$, $l = 10$, $v = 0.01$, $U_k^p = 0.01$, and pulses (of duration $\delta t = 10 \times dt$) after every $T = 1000 \times dt$ duration on the kth ($= 50$) block.
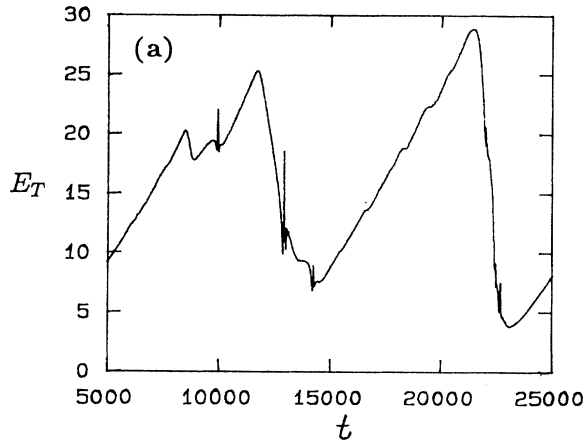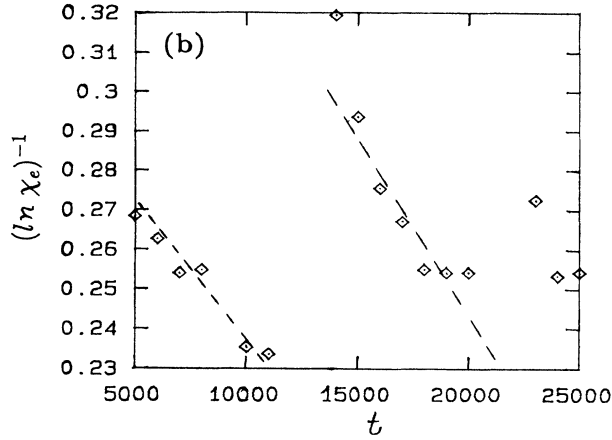
FIG. 7. A close view of the time variation of (a) total elastic energy E_T and (b) $(\ln \chi_e)^{-1}$. Here, $N = 100$, $\alpha = 2.5$, $l = 10$, $v = 0.01$, $U_f^0 = 0.01$, and pulses (of duration $\delta t = 10 \times dt$) after every $T = 1000 \times dt$ duration on the kth ($= 50$) block.
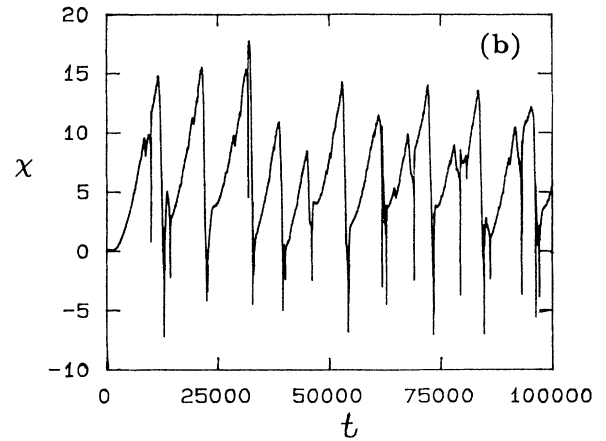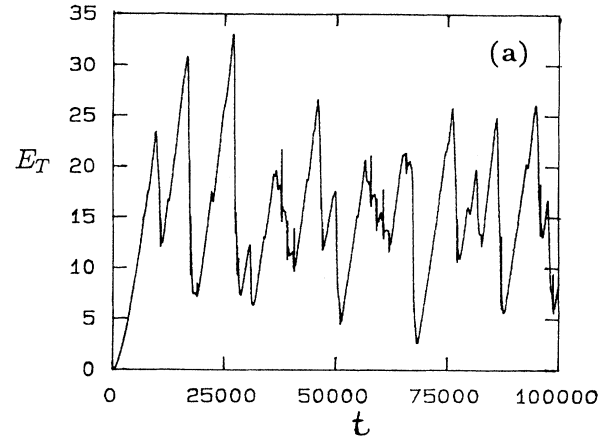
FIG. 8. Time variation of (a) total elastic energy E_T and (b) susceptibility χ for the unperturbed (by pulses) system. Here $N = 100$, $\alpha = 2.5$, $l = 10$, and $v = 0.01$.

(unperturbed case) can be summed up to give a direct susceptibility $\chi(t)$ (with $\chi = \sum_r g(r)$, where $g(r) = \langle \Delta U_0 \Delta U_r \rangle$, with $\Delta U_j [= l^2(U_{j+1} - 2U_j + U_{j+1}) - U_j]$ denoting the stress on the jth block in the model [7]). The behavior of this susceptibility exactly matches with our previously obtained results for χ_e [10] in that it also grows exponentially with time and diverges at the "earthquake" points or times (see Fig. 8). In fact, the finite height of the peak in χ (or χ_e) is observed to be a finite size effect. In Fig. 9 we show the χ variation in time for the same dynamical parameter values for two different system sizes, i.e., $N = 100$ and $N = 200$. The figure there shows that the peak height in χ indeed grows with N and diverges to infinity at $N \to \infty$. This also indicates that the study of the response to the local pulses indeed helps to estimate the growing stress (and consequent slip) correlations in the system.

In Fig. 10, we show the distribution $\rho(E)$ of earthquakes releasing energy E. The distribution indeed follows the Guttenberge-Richter type of power law decay $[\rho(E) \sim E^{-\beta}, \beta \sim 1.2]$ [7], both in the unperturbed system (without pulse) and the system perturbed by weak pulses

(on the kth block) at regular intervals. In may be noted, however, although the nature of the distribution remains unchanged, because of the sensitivity of the initial conditions the exact magnitude and timings of the quakes are somewhat different in the two cases (pulsed and unperturbed). To sense the growing correlations in the system, one needs to study the response of the system to (very weak) pulsed perturbations, which, however, affect the time sequence of the events (of course, keeping the distribution and the exponent unchanged). One therefore has to apply the pulse periodically and measure the susceptibility of the system at regular intervals to look for its critical growth just before the (global) earthquake.

V. CONCLUDING REMARKS

Extensive research for the last decade or so has helped in the development of several simple models [2,3,6,11] for the study of breakdowns (fractures, dielectric breakdowns, avalanches, or earthquakes) in randomly disordered media or systems. Established properties of the breakdown strength distribution in such systems (and the absence of full-grown chaos in the breakdown dynamics)
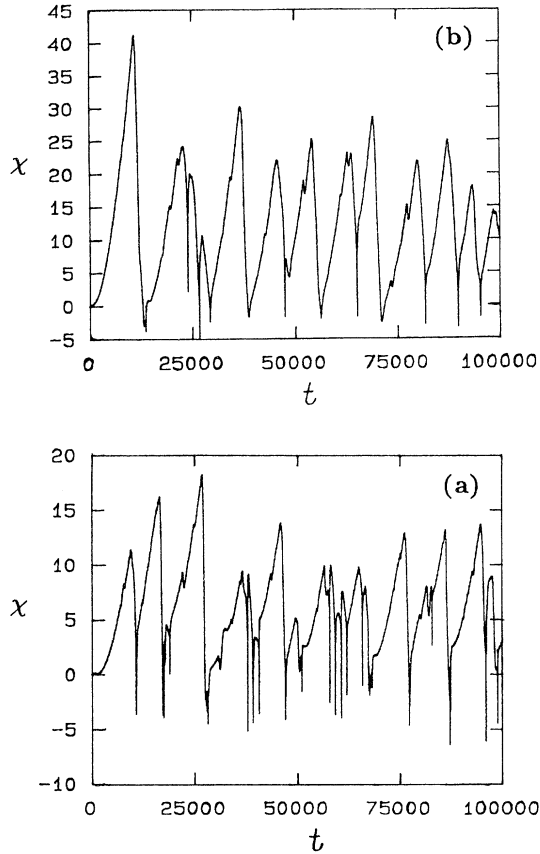
FIG. 9. Time variation of χ (unperturbed) for different system sizes. (a) $N=100$; (b) $N=200$, with fixed $\alpha=2.5$, $l=10$, and $v=0.01$.

FIG. 10. Distribution $\rho(E)$ of total elastic energy E released during earthquakes in the model, both unperturbed and perturbed (with pulse) cases. $N=100$, $\alpha=2.5$, $l=10$, and $v=0.01$.

indicated the possible growth of local failure correlations [10] in such systems as the global breakdown point is approached. This, in turn, suggested the study of appropriate (breakdown) susceptibility, whose growth could be taken as the precursor of the macroscopic or global catastrophes. It may be noted that there have also been indications [15] that some other linear properties (e.g., the ratio of shear modulus and bulk modulus, obtainable from sound velocity measurements) show abnormal (but universal) properties near the breakdown (macroscopic fracture) points of disordered solids. The detailed study of such a (linear) response (before breakdown) has been shown to provide an advance indication of the imminent (macroscopic) failure in the case of fractures in random elastic media. Such methods (for extracting advance information) are also quite "nondestructive." However, such indications are found to be very selective, and it has not been possible yet to use them for the study of prior indications in all the important cases of catastrophic failures like earthquakes. It appears that although somewhat "destructive" in nature and perhaps also hard to measure experimentally, the growing response (from local failure correlations) to short pulses or some additional applied field is, at least in various theoretical models of breakdown, quite generic and ubiquitous.
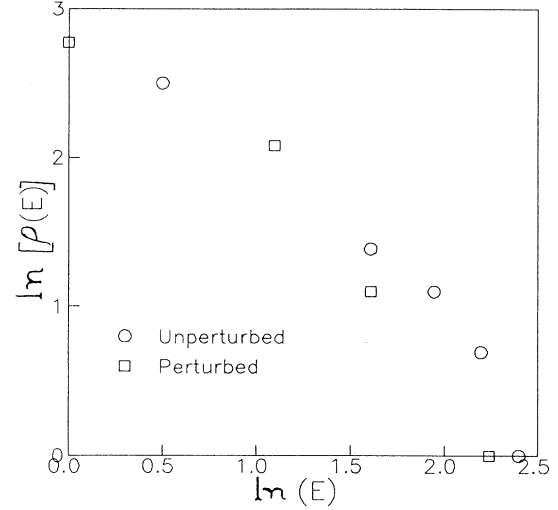
Here we have reported in detail the results of the study of the response to appropriate short-duration and local pulsed perturbations on such systems. It has been shown that appropriate (breakdown) susceptibility (linear ratio of the response to the perturbation amplitudes or widths) senses very accurately the growing (local failure) correlations in the system as the system approaches its global breakdown point. Specifically, we have studied the responses to short-duration pulses (of electric field, of additional particles, of mechanical "push" on any "tectonic block," etc.) for metal-insulator composites before dielectric breakdown, the BTW (sandpile) model before the critical avalanches, and the Burridge-Knopoff stick-slip model of earthquakes. The study of the breakdown susceptibility indicates universal behavior near the catastrophic breakdown or the self-organized critical points. Specifically, we have made a numerical study of Laplace's equation of a dielectric with random bond conductors below its percolation threshold, the dynamics of the BTW model, and the dynamical equation of the array of blocks in the stick-slip model of earthquakes, all in the presence of appropriate pulsed perturbations. We show that one can estimate the growth of local failure correlations from the response to such pulsed perturbations, giving the breakdown susceptibility. Studies of these breakdown susceptibilities are shown to help in accurately locating the global breakdown or disaster point (much before its occurrence) by extrapolating, to its vanishing point, the inverse breakdown susceptibility. The breakdown susceptibility has a power law growth (with the critical interval from the global breakdown threshold) in both electric breakdown and in the BTW model. Accurate exponent values for the growth have been obtained in the BTW case. The growth of the susceptibility, coming from stress correlations, in the Burridge-Knopoff

model of earthquakes is observed to be exponential in time, as it is for pulse susceptibility in the same model.

In summary, we find that one can define appropriate susceptibilities for systems having macroscopic breakdown properties. As the (global) breakdown point approaches (for example, by increasing the external voltage across random dielectrics or with the increase of time, as in the BTW sandpile model or in the Burridge-Knopoff model of earthquakes), the appropriate correlations grow and the corresponding susceptibility tends to diverge at the disaster point. By investigating, therefore, the nature

of such susceptibility and by locating the extrapolated point where its inverse vanishes, one can make predictions about the imminent breakdown point.

[1] See, e.g., *Nonlinearity and Breakdown in Soft Condensed Matter*, edited by K. K. Bardhan, B. K. Chakrabarti, and A. Hansen, Lecture Notes in Physics Vol. 437 (Springer-Verlag, Heidelberg, 1994).

[2] R. Ray and B. K. Chakrabarti, J. Phys. C **18**, L185 (1985); B. K. Chakrabarti, D. Chowdhury, and D. Stauffer, Z. Phys. B **62**, 343 (1986); M. Sahimi and J. D. Goddard, Phys. Rev. B **33**, 7848 (1986); M. Sahimi and S. Arbabi, *ibid.* **47**, 713 (1993); B. K. Chakrabarti, in *Nonlinearity and Breakdown in Soft Condensed Matter* (Ref. [1]), pp. 171–185.

[3] L. de Arcangelis, S. Redner, and H. J. Herrman, J. Phys. (Paris) Lett. **46**, L585 (1985); P. M. Duxbury, P. D. Beale, and P. L. Leath, Phys. Rev. Lett. **57**, 1052 (1986); P. M. Duxbury, P. L. Leath, and P. D. Beale, Phys. Rev. B **36**, 367 (1987); P. D. Beale and J. D. Srolovitz, *ibid.* **37**, 5500 (1988); P. M. Duxbury and P. L. Leath, Phys. Rev. Lett. **72**, 2805 (1994); P. L. Leath, in *Nonlinearity and Breakdown in Soft Condensed Matter* (Ref. [1]), pp. 151–170.

[4] L. Benguigui, P. Ron, and D. J. Bergman, J. Phys. (Paris) **48**, 1547 (1987); K. Seiradzki and R. Li, Phys. Rev. Lett. **56**, 2509 (1986); L. Benguigui, Phys. Rev. B **38**, 7211 (1988); R. Li and K. Seiradzki, Phys. Rev. Lett. **68**, 1168 (1992); L. Benguigui and P. Ron, in *Nonlinearity and Breakdown in Soft Condensed Matter* (Ref. [1]), pp. 221–234.

[5] M. Marder, Phys. Rev. E **49**, R51 (1994); R. M. Bradley

and K. Wu, J. Phys. A **26**, 327 (1993); K. Wu and R. M. Bradley, Phys. Rev. E **50**, R631 (1994); Phys. Rev. B **50**, 12 468 (1994).

[6] R. Burridge and L. Knopoff, Bull. Seismol. Soc. Am. **57**, 341 (1967).

[7] J. M. Carlson and J. S. Langer, Phys. Rev. Lett. **62**, 2632 (1989); Phys. Rev. A **40**, 6470 (1989); M. de Sousa Viera, G. L. Vasconcelos, and S. R. Nagel, Phys. Rev. E **47**, 2221 (1993); J. P. Vilotte, J. Schmitthul, and S. Roux, in *Nonlinearity and Breakdown in Soft Condensed Matter* (Ref. [1]), pp. 54–77; G. Ananthakrishna and H. Ramachandran, in *Nonlinearity and Breakdown in Soft Condensed Matter* (Ref. [1]), pp. 78–106; J. M. Carlson, J. S. Langer, and B. E. Shaw, Rev. Mod. Phys. **66**, 657 (1994).

[8] A. Yuse and M. Sano, Nature (London) **362**, 329 (1993).

[9] J. S. Langer, Phys. Rev. Lett. **70**, 3592 (1993).

[10] M. Acharyya and B. K. Chakrabarti, J. Phys. (France) I **5**, 153 (1995); Ind. J. Phys. A **69**, 205 (1995).

[11] P. Bak, C. Tang, and K. Wiesenfeld, Phys Rev. Lett. **59**, 381 (1987).

[12] S. S. Manna and B. K. Chakrabarti, Phys. Rev. B **36**, 4078 (1987); see also P. D. Beale and P. M. Duxbury, *ibid.* **37**, 2785 (1988).

[13] D. Stauffer and A. Aharony, *Introduction to Percolation Theory* (Taylor & Francis, London, 1992).

[14] S. S. Manna, J. Stat. Phys. **59**, 509 (1990).

[15] M. Sahimi and S. Arbabi, Phys. Rev. Lett. **68**, 608 (1992).